



Submitted to

XVIII International Workshop on Deep-Inelastic Scattering, DIS2010, April 19-23, 2010, Florence

Parallel Session **Electroweak and Searches in DIS and Hadron Colliders**

Electronic Access: www-h1.desy.de/h1/www/publications/conf/confList.html

Search for Squarks in R-Parity Violating Supersymmetry at HERA.

H1 Collaboration

Abstract

A search for squarks in R -parity violating supersymmetry is performed in $e^\pm p$ collisions at HERA using the H1 detector. The full data sample taken at a centre-of-mass energy $\sqrt{s} = 319$ GeV is used for the analysis, corresponding to an integrated luminosity of 438 pb^{-1} . The resonant production of squarks via a Yukawa coupling λ' is considered, taking into account direct and indirect R -parity violating decay modes. No evidence for squark production is found in the (multi-)lepton and (multi-)jet final state topologies investigated. Mass dependent limits on λ' are obtained in the framework of the Minimal Supersymmetric Standard Model and in the minimal Supergravity Model. In the considered part of the parameter space, for a Yukawa-type coupling of electromagnetic strength $\lambda' = 0.3$, squarks of all flavours are excluded up to masses of 275 GeV at 95% confidence level, with down-type squarks further excluded up to masses of 290 GeV.

Search for Squarks in RPV SUSY with H1 (Preliminary)						
Channel	$e^+ p$ (255 pb $^{-1}$)		$e^- p$ (183 pb $^{-1}$)		Signal Efficiency	
	Data	SM Expectation	Data	SM Expectation		
eq	2946	2899 ± 302	3121	3215 ± 336	30 – 40%	
νq	-	-	2858	2983 ± 358	50 – 60%	
eMJ (RC)	140	145.6 ± 21.3	147	157.7 ± 23.8	10 – 40%	
eMJ (WC)	1	0.6 ± 0.4	0	1.3 ± 0.3	5 – 20%	
νMJ	19	23.4 ± 5.8	24	28.9 ± 7.2	5 – 15%	
$eeMJ$	2	1.7 ± 0.5	0	1.5 ± 0.5	5 – 35%	
$e\mu MJ$	0	0.03 ± 0.03	0	0.03 ± 0.02	5 – 15%	
$\nu e MJ$	5	8.2 ± 2.0	3	5.6 ± 1.2	5 – 40%	
$\nu \mu MJ$	0	0.06 ± 0.03	0	0.04 ± 0.02	5 – 20%	

Table 1: Total numbers of selected events, SM expectation and ranges of selection efficiencies for the squark decay channels considered in the analysis of 255pb $^{-1}$ $e^+ p$ and in 183pb $^{-1}$ $e^- p$ collision data. The range of signal efficiencies gives the extreme values for squark masses ranging from 100 GeV to 290 GeV and gaugino masses 30 GeV up to the squark mass. The \tilde{u}_L -type squarks ($e^+ p$ collisions) cannot decay to νq . The total error on the SM prediction is determined by adding the effects of all model and experimental systematic uncertainties in quadrature.

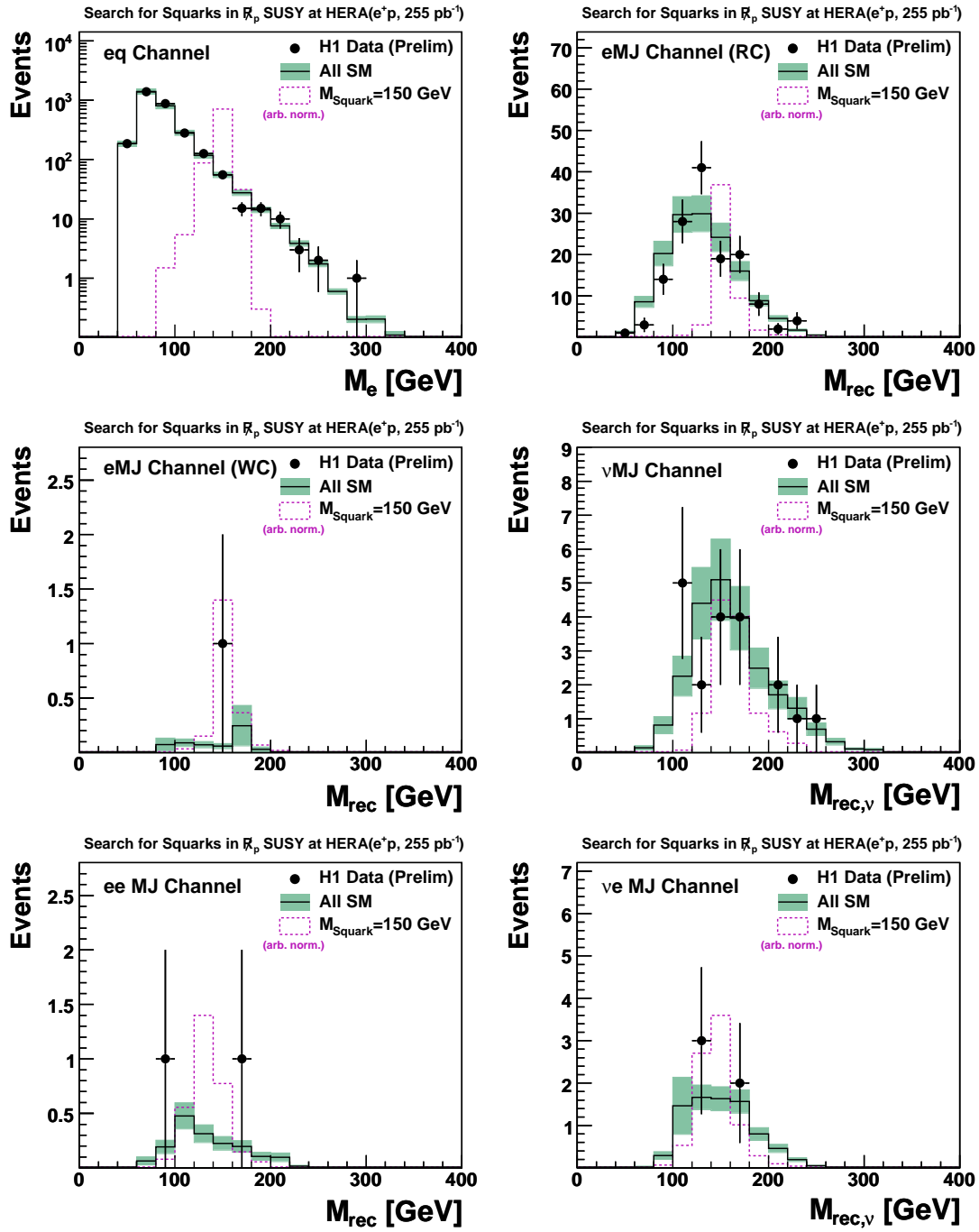


Figure 1: Invariant mass distributions in all selection channels with data (points) events in e^+p data. The method used for the reconstruction ($M_e, M_h, M_{rec}, M_{rec,\nu}$) depends on the analysis channel. The error band gives all model and experimental systematic uncertainties on the SM prediction (solid histogram) added in quadrature. The dashed histogram indicates the signal from a squark with $m_{\tilde{q}} = 150$ GeV in arbitrary normalisation.

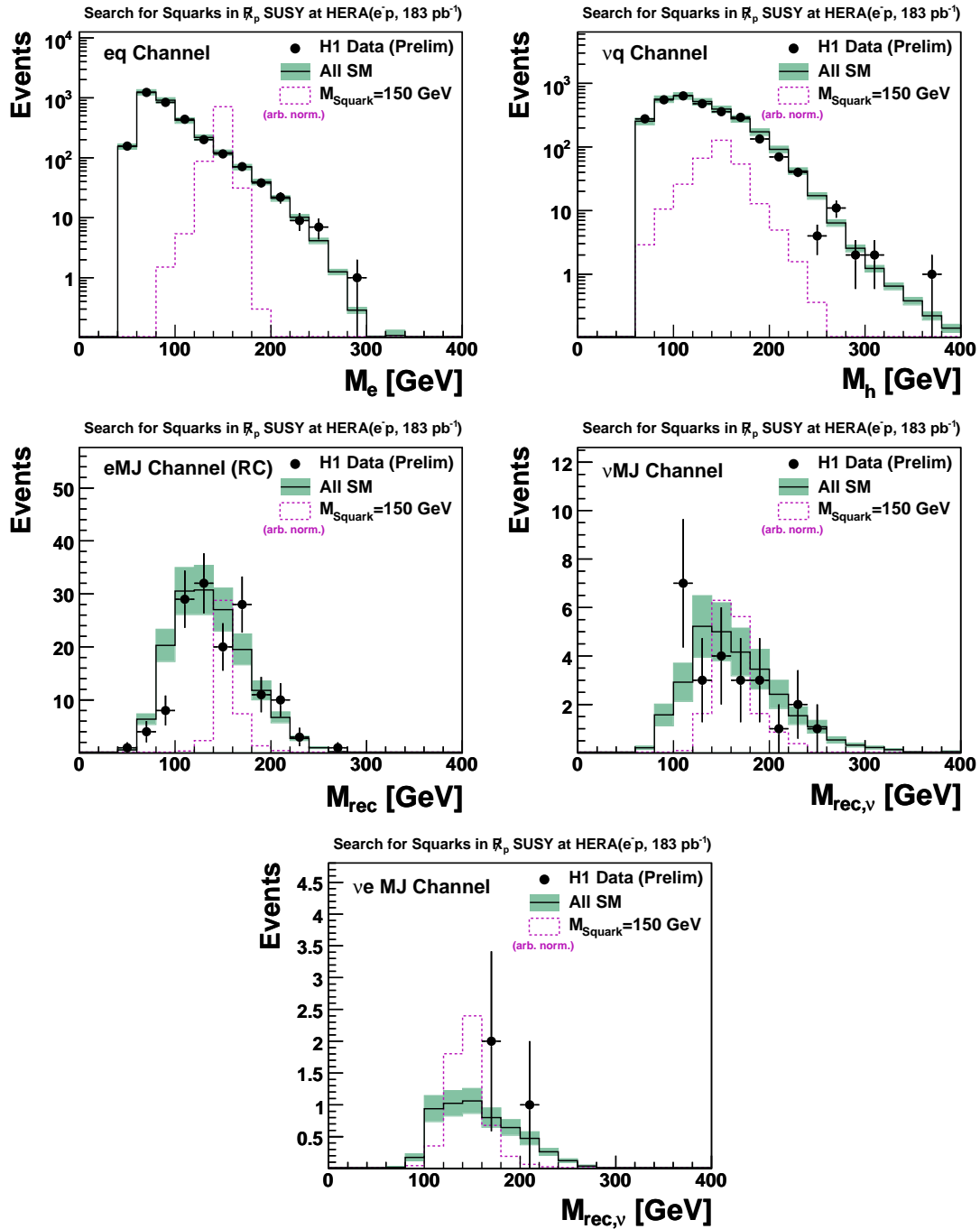


Figure 2: Invariant mass distributions in all selection channels with data (points) events in $e^- p$ data. The method used for the reconstruction ($M_e, M_h, M_{rec}, M_{rec,\nu}$) depends on the analysis channel. The error band gives all model and experimental systematic uncertainties on the SM prediction (solid histogram) added in quadrature. The dashed histogram indicates the signal from a squark with $m_{\tilde{q}} = 150$ GeV in arbitrary normalisation.

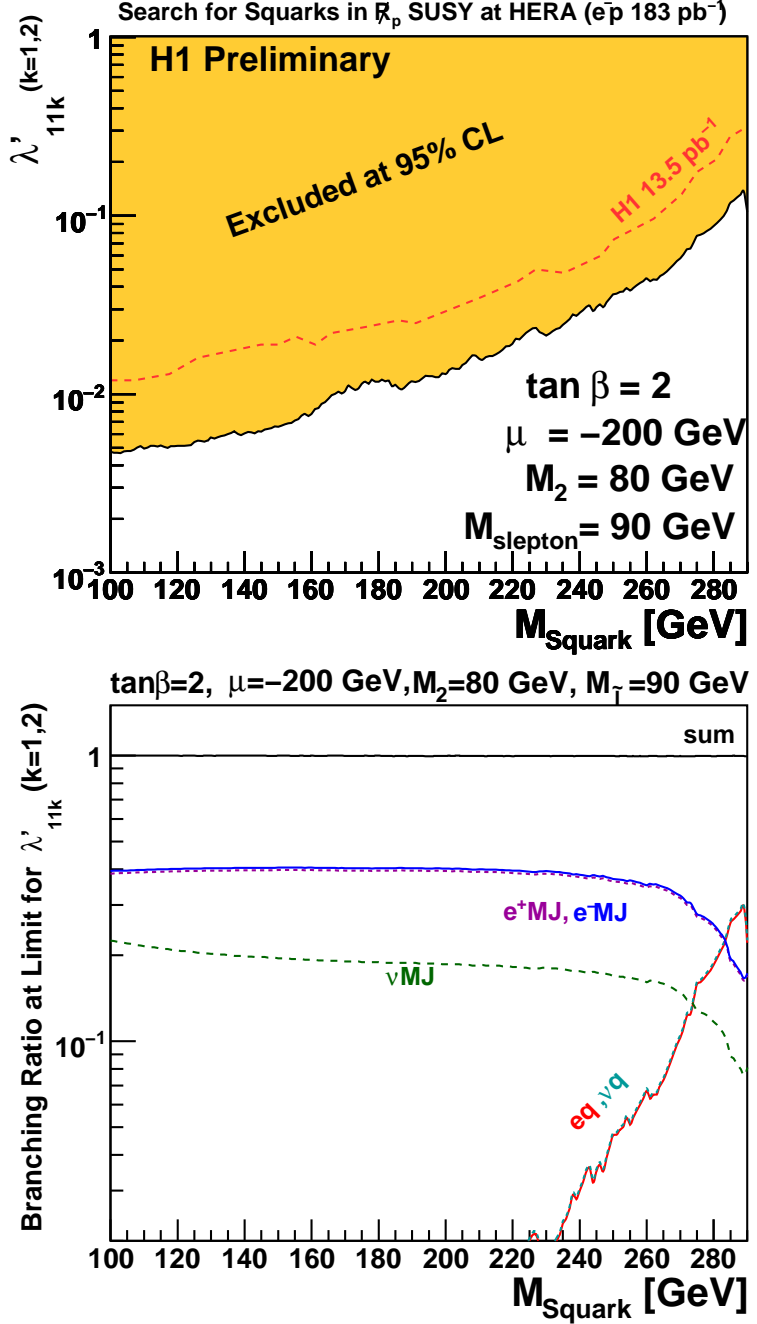


Figure 3: In a phenomenological MSSM with a photino ($\tilde{\gamma}$) like neutralino $\tilde{\chi}_1^0$ exclusion limits at 95% CL on λ'_{11k} ($k = 1, 2$). A slepton mass of 90 GeV is assumed. For comparison, the corresponding limit from the HERA I analysis is also indicated. (b) Branching ratios to the decay channels considered in this analysis for λ' values at the observed limit.

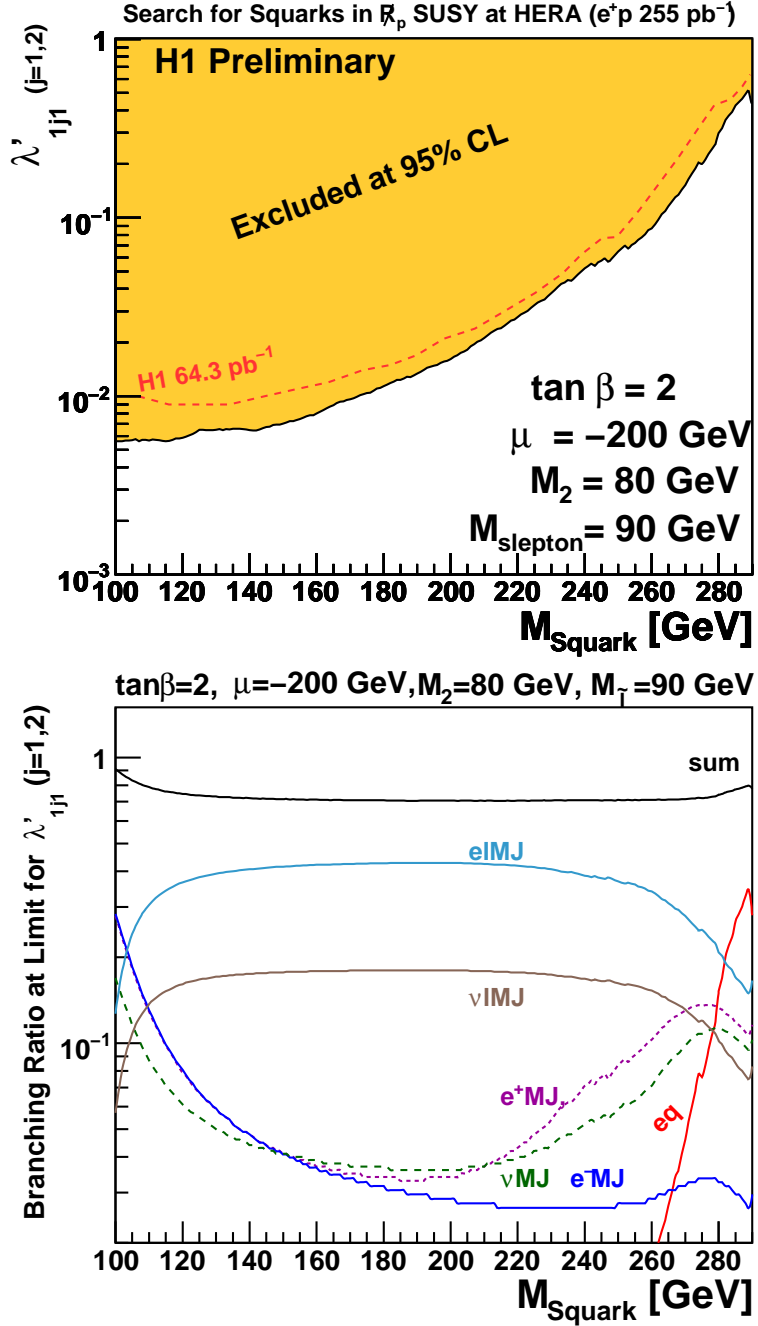


Figure 4: In a phenomenological MSSM with a photino ($\tilde{\gamma}$) like neutralino χ_1^0 exclusion limits at 95% CL on λ'_{1j_1} ($j = 1, 2$). A slepton mass of 90 GeV is assumed. For comparison, the corresponding limit from the HERA I analysis is also indicated. (b) Branching ratios to the decay channels considered in this analysis for λ' values at the observed limit.

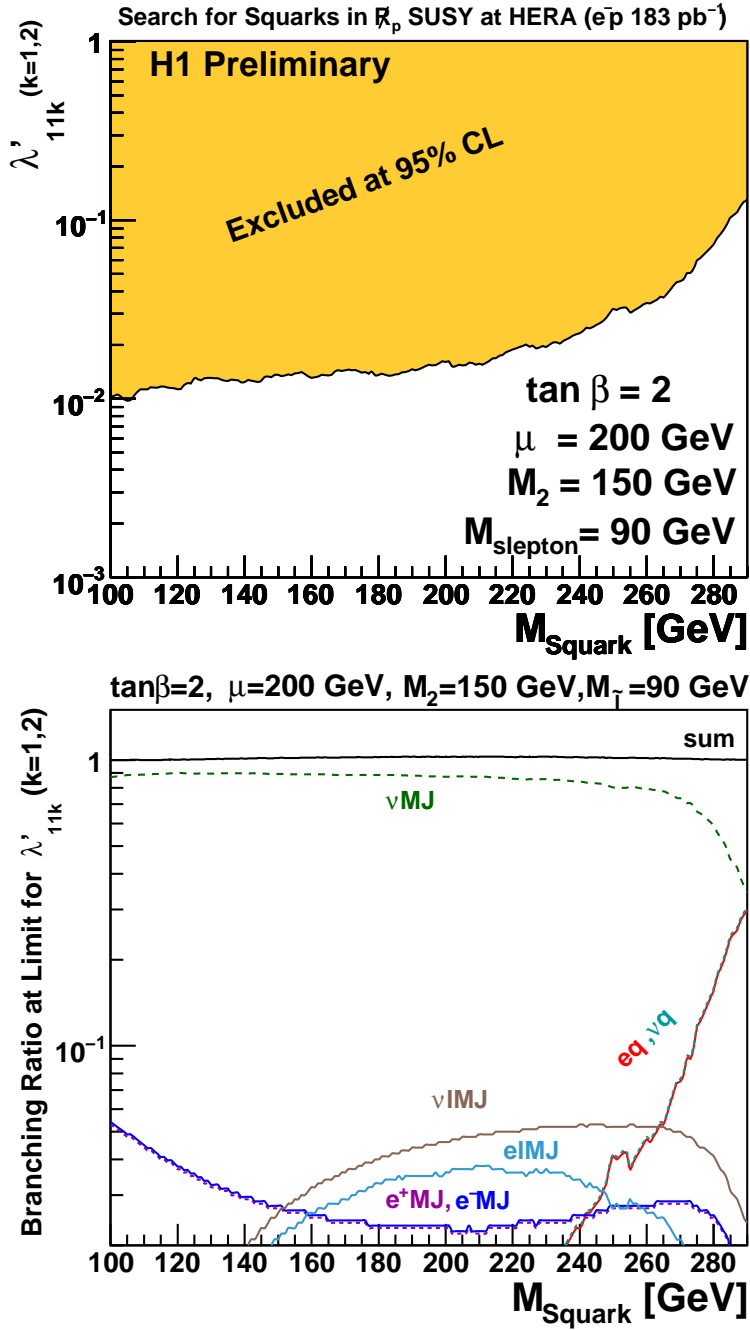


Figure 5: In a phenomenological MSSM with a zino (\tilde{Z}) like neutralino χ_1^0 (a) exclusion limits at 95% CL on λ'_{11k} ($k = 1, 2$). A slepton mass of 90 GeV is assumed. (b) Branching ratios to the decay channels considered in this analysis for λ' values at the observed limit.

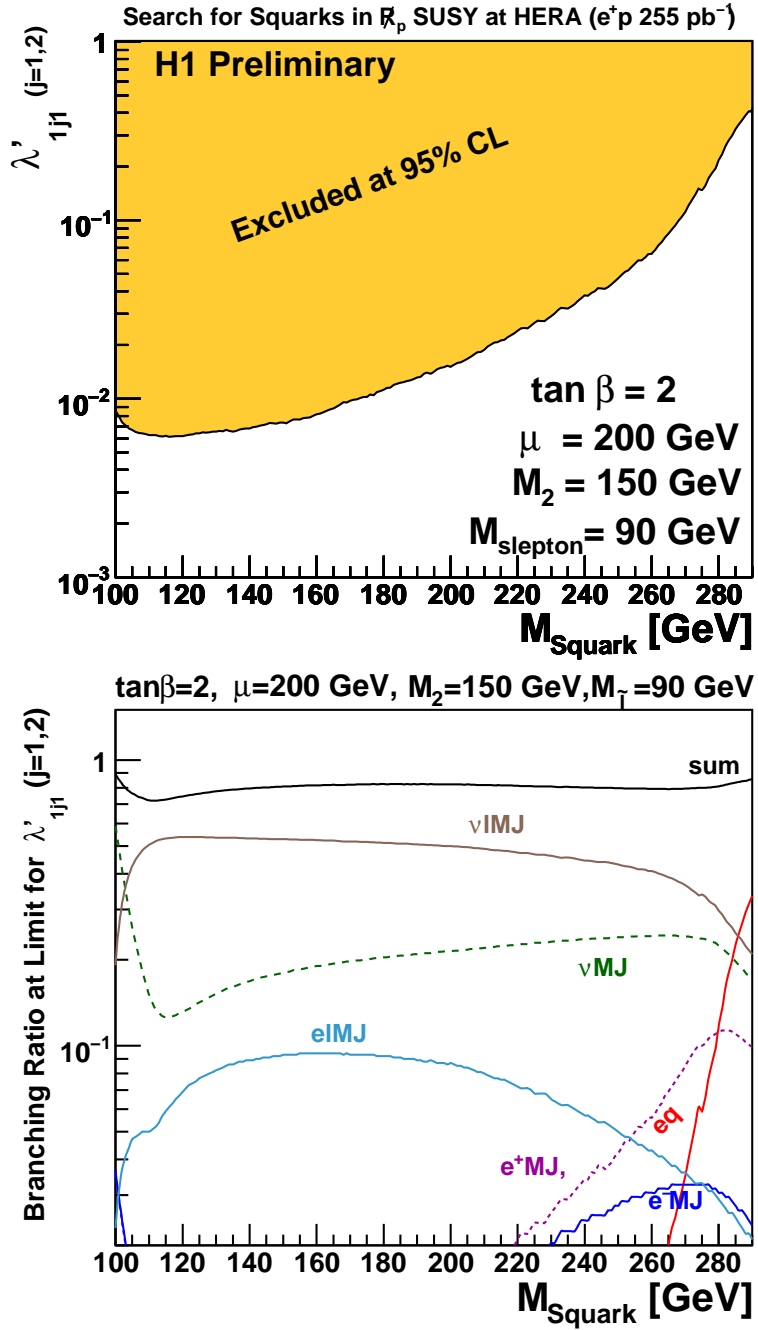


Figure 6: In a phenomenological MSSM with a zino (\tilde{Z}) like neutralino χ_1^0 (a) exclusion limits at 95% CL on $\lambda'_{1j_1} (j = 1, 2)$. A slepton mass of 90 GeV is assumed. (b) Branching ratios to the decay channels considered in this analysis for λ' values at the observed limit.

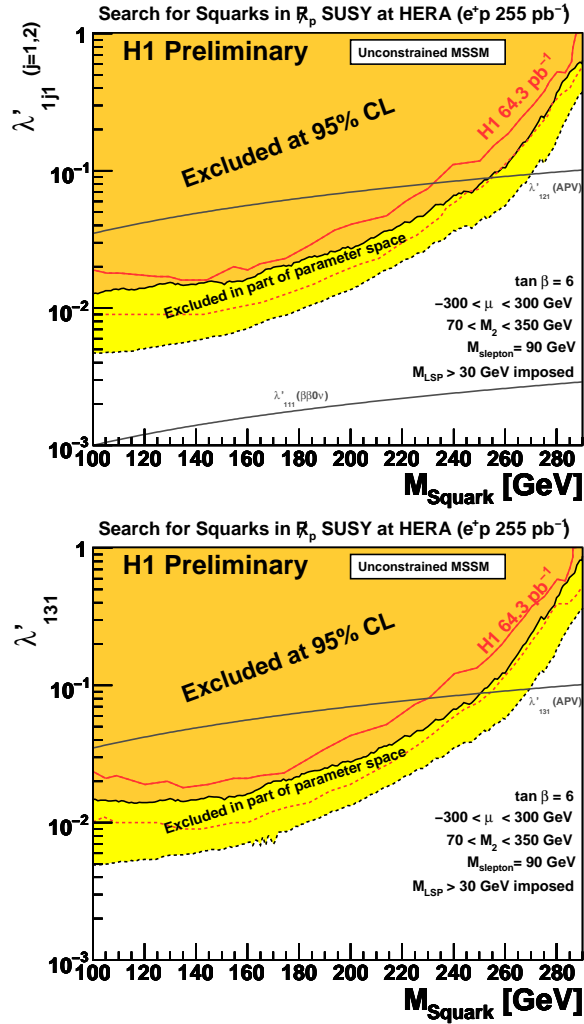


Figure 7: Exclusion limits at 95 % CL on λ'_{1j1} for (a) $j = 1, 2$ and (b) $j = 3$ as a function of the squark mass from a scan of the MSSM parameter space as indicated in the figures. Values of λ' higher than the solid curve could be excluded in all scenarios, values in between the solid and the dashed curve could be excluded in part of the parameter space investigated. Indirect limits from neutrinoless double beta decay experiments ($\beta\beta0\nu$) and atomic parity violation (APV) are also shown. For comparison, the corresponding limit from the HERA I analysis is also indicated.

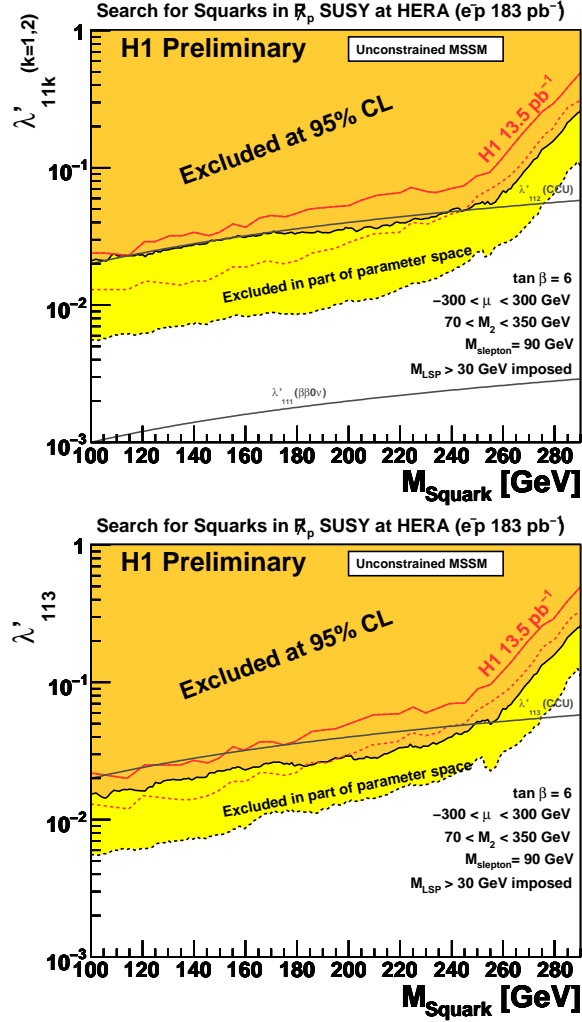


Figure 8: Exclusion limits at 95 % CL on λ'_{11k} for (a) $k = 1, 2$ and (b) $k = 3$ as a function of the squark mass from a scan of the MSSM parameter space. Values of λ' higher than the solid curve could be excluded in all scenarios, values in between the solid and the dashed curve could be excluded in part of the parameter space investigated. Indirect limits from neutrinoless double beta decay experiments ($\beta\beta 0\nu$) and tests of charged current universality (CCU) are also shown. For comparison, the corresponding limit from the HERA I analysis is also indicated.

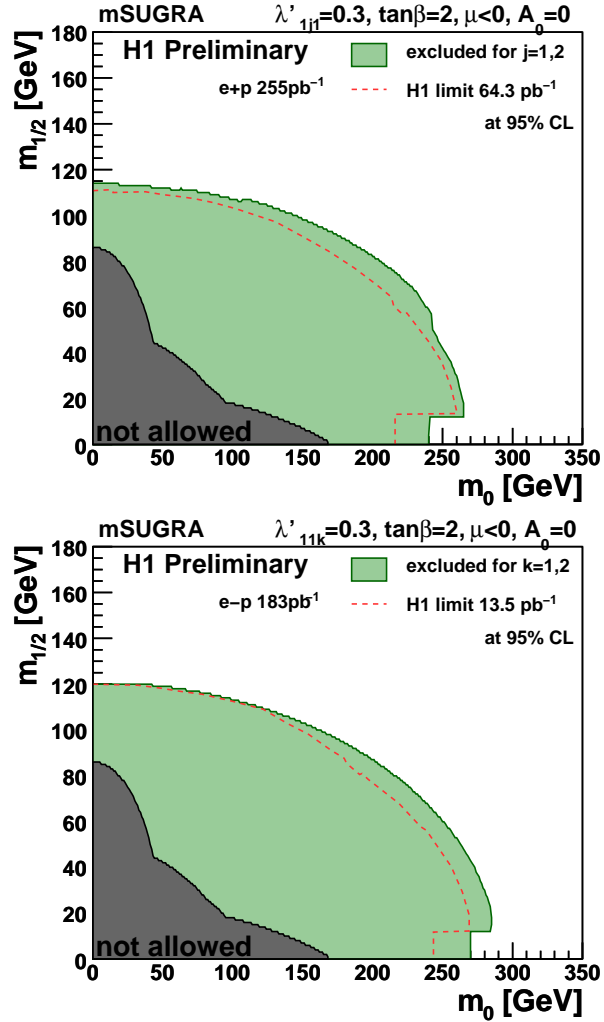


Figure 9: Exclusion limits at 95 % CL in the $m_0, m_{1/2}$ plane assuming (a) $\lambda'_{1j1} = 0.3$ for $j = 1, 2$ and (b) $\lambda'_{11k} = 0.3$ for $k = 1, 2$. The corresponding limit from the HERA I analysis is also indicated.

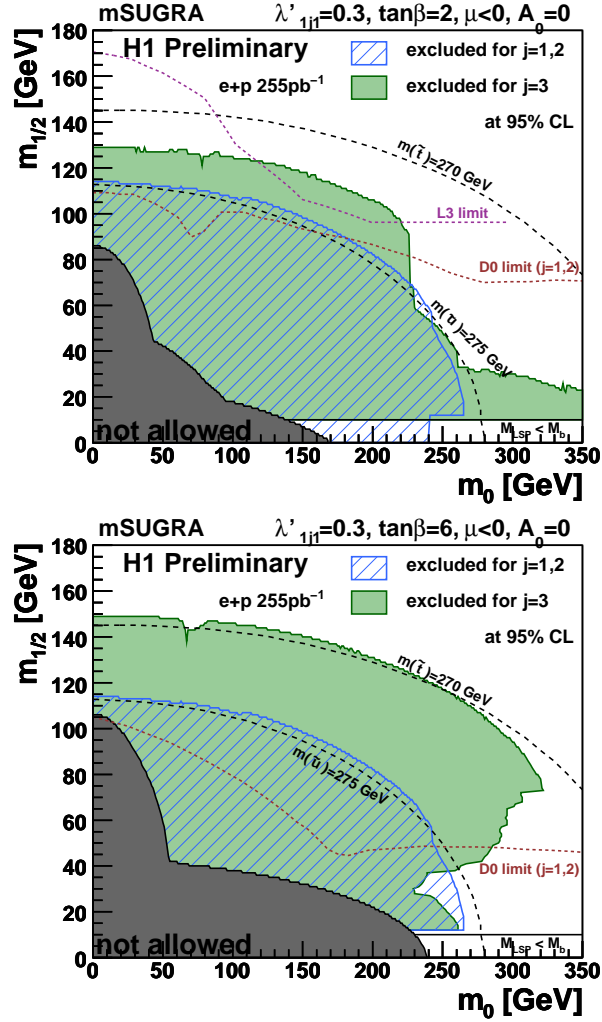


Figure 10: Exclusion limits at 95 % CL in the $m_0, m_{1/2}$ plane assuming $\lambda'_{1j1} = 0.3$ for (a) $\tan\beta = 2$ (b) $\tan\beta = 6$ for $j = 1, 2$ hatched blue and $j = 3$ filled green. Curves of constant squark mass are illustrated for $m(\tilde{u}) = 275$ GeV and $m(\tilde{t}) = 270$ GeV. Constraints obtained by the L3 experiment at LEP and D0 experiment at the Tevatron are also indicated.

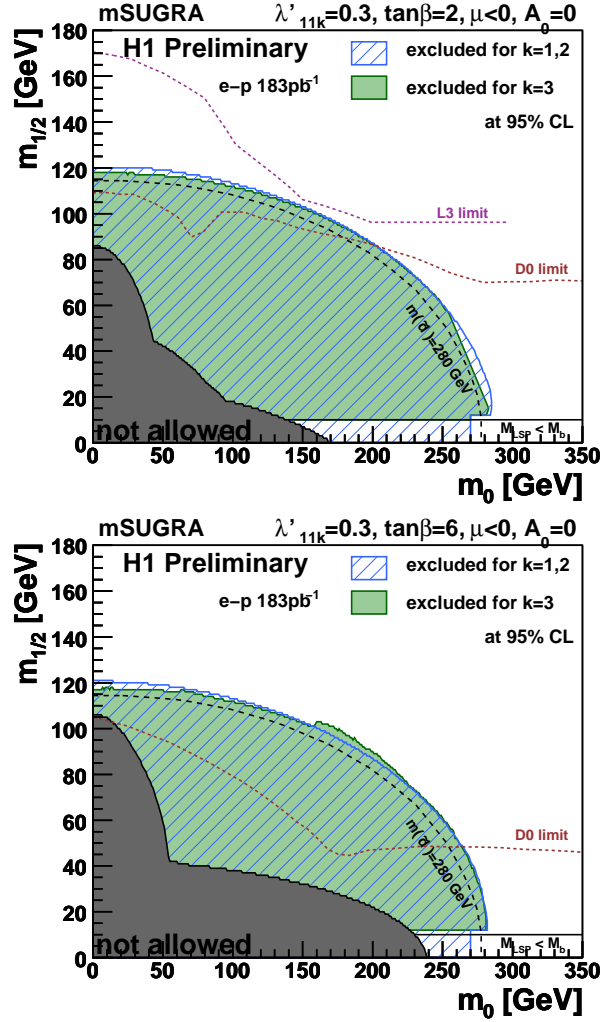


Figure 11: Exclusion limits at 95 % CL in the $m_0, m_{1/2}$ plane assuming $\lambda'_{11k} = 0.3$ for (a) $\tan\beta = 2$ (b) $\tan\beta = 6$ for $k = 1, 2$ hatched blue and $k = 3$ filled green. A curve of constant squark mass is illustrated for $m(\tilde{d}) = 280$ GeV. Constraints obtained by the L3 experiment at LEP and D0 experiment at the Tevatron are also indicated.

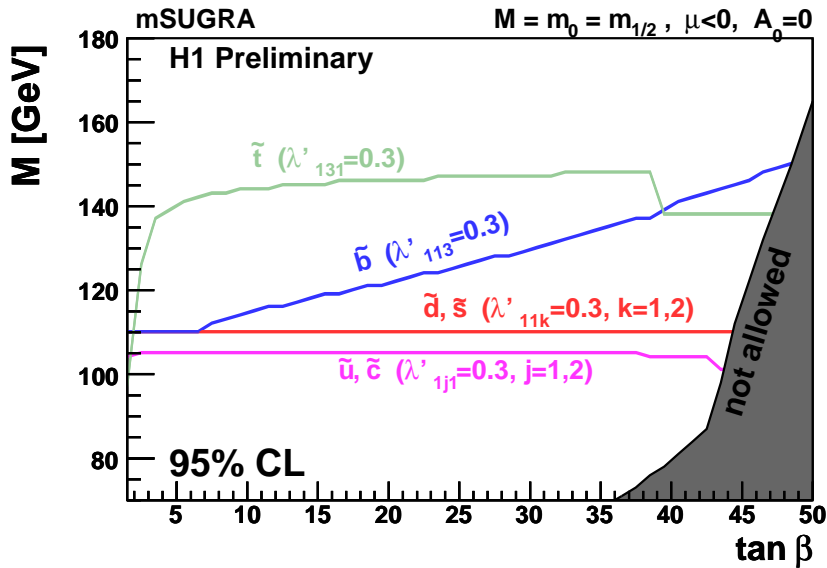


Figure 12: Exclusion limits for $m_0 = m_{1/2} = M$ in the mSUGRA model as a function of $\tan \beta$. Shown are the 95 % CL exclusion limits for $\lambda'_{1jk} = 0.3$. The area below the curves is excluded. The dark region corresponds to values of parameters where REWSB is not possible or the LSP is a sfermion.